Chapter 2

ESR Spectroscopy of Nitroxides: Kinetics and Dynamics of Exchange Reactions

Günter Grampp and Kenneth Rasmussen

Additional information is available at the end of the chapter

http://dx.doi.org/10.5772/39131

1. Introduction

Stable nitroxide radicals have proved to be helpful in solving many problems in chemistry, biochemistry, biophysics, material science etc. as model compounds. To understand in detail the great variety of different chemical reactions, a good knowledge of the underlying "simple" exchange reactions related to nitroxide radicals is necessary. This chapter focuses on electron-self and spin exchange reactions of various nitroxide radicals in different solvents. The corresponding rate constants, the activation parameters, like activation enthalpies and volumes are obtained from temperature- and pressure dependent ESR-line broadening effects. A short introduction to dynamic ESR-spectroscopy is given.

1.1. From ESR spectrum to exchange rate constant

There are several chemical reactions giving rise to dynamic line shape effects, such as spin-exchange, also known as Heisenberg exchange, electron self-exchange and proton or counter ion transfer. A theoretical illustration of how an ESR spectrum may be affected by chemical reactions is presented in figure 1. Here, the interconvertion between two states, a and b, can influence the spectrum dramatically as the exchange rate increases.

Apart from the two extreme limits of infinitely slow or fast exchange, usually three regions are considered: slow, intermediate and fast. In the slow region the two lines broaden as if the life, or relaxation, times of the spins had been reduced due to quenching. When the exchange enters the intermediate region, the interconvertion rate leads to an averaging of the lines and correspondingly to line shifts. At one point, the exchange so fast that the spectrum appears as a single line due to overlap of the two original ones. This marks the beginning of the fast region, where a further increase in the exchange rate leads to narrowing of the single line.

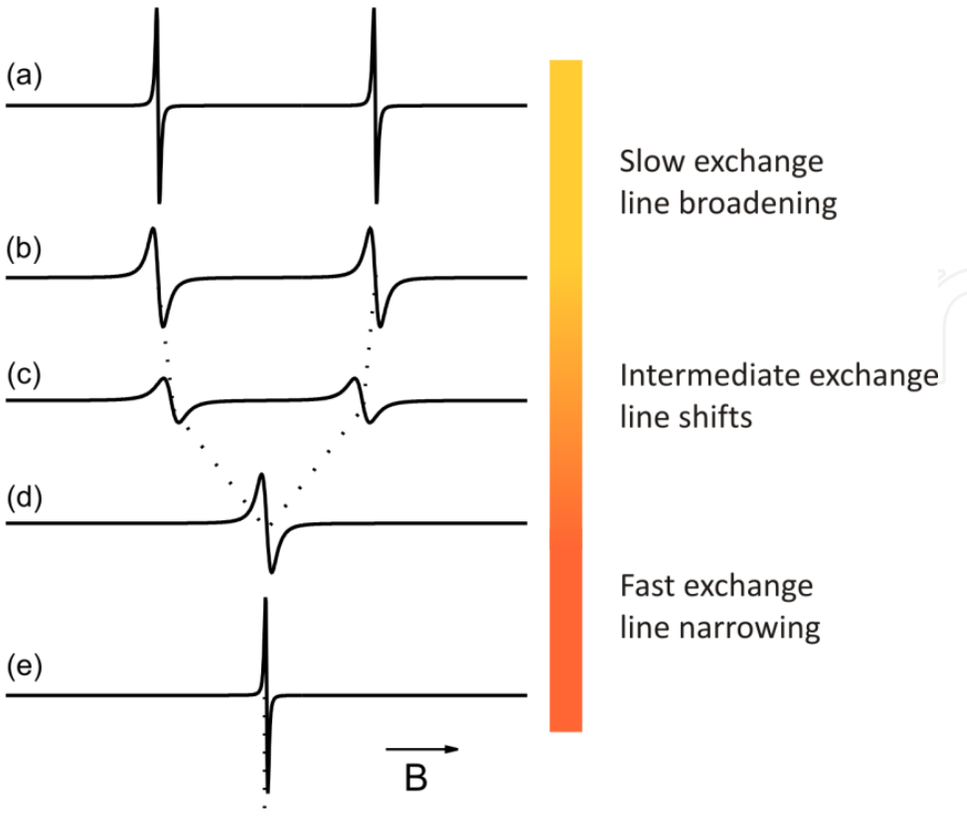

Figure 1. Theoretical illustration of the first derivative ESR spectra arising from the interconversion between forms *a* and *b*. (a) Slow limit. (b) Moderately slow region. (c) Intermediate region showing line shifts. (d) Moderately fast region. (e) Fast limit.

A chemical reaction corresponding to this illustration could, for example, be an exchange reaction like the one shown in equation (1), where the forms *a* and *b* are interpreted as being molecules having different nuclear spin configurations.

$$A_{(a)} + A^{\bullet -}_{(b)} \xrightarrow{k_{obs}} A^{\bullet -}_{(a)} + A_{(b)} \tag{1}$$

Transferring the unpaired electron from one molecule to the other thus corresponds to the interchange between the two forms. Note, that reactions between molecules of the same form, e.g. *a*, also take place. If this happens no ESR line broadening is expected, but nevertheless the electron transfer takes place and these 'uneventful' reactions must be taken into account. The resulting line width in the case of slow exchange then becomes:

$$\Delta B = \Delta B^{o} + \frac{1 - p_j}{\left|\gamma_e \tau\right|} \tag{2}$$

with p_j being the probability that the reactants have the same nuclear spin configuration, here *j*.

In general, an ESR spectrum may show more than just a few lines (states), of which some are originating from transitions involving degenerate energy levels. This can give rise to

substantially different values of p_j and it is important to recognize that when a self-exchange reaction occurs, one expects the ESR lines to have different widths. Strictly speaking, equation (2) is therefore only valid for a single state and its corresponding ESR line.

Looking at equation (1) from the point of view of chemical kinetics it is seen that although the self-exchange reaction is bimolecular, one may express it using a first order rate law since the concentration of diamagnetic species is constant. Recalling the relationship between life times and first order rate constants one obtains

$$\tau = \frac{1}{k} = \frac{1}{k_{obs}[A]} \tag{3}$$

which in combination with equation (2) and taking the ESR signal in its first derivative Lorentzian form results in the following relationship between line broadening and rate constant:

$$k_{obs} = \frac{\sqrt{3}\pi\left|\gamma_e\right|\left(\Delta B_{pp} - \Delta B_{pp}^{o}\right)}{\left(1-p_j\right)\left[A\right]} \tag{4}$$

where ΔB_{pp}^{o} and ΔB_{pp} are the peak-to-peak widths of the first derivative line in the absence and presence of the self-exchange reaction.

Similarly, an expression of k_{obs} may be derived for the fast exchange region, where the broadening of the singe ESR line obeys

$$\left(\Delta B_{pp} - \Delta B_{pp}^{o}\right) = \frac{4\pi\left|\gamma_e\right|\nabla_2}{3k_{obs}\left[A\right]} \tag{5}$$

Here ∇_2 is the second moment of the ESR spectrum, that is

$$\nabla_2 = \sum_j p_j\left(\overline{B} - B_j\right)^2 \tag{6}$$

with $\overline{B}$ being the center field of the spectrum and B_j the resonant magnetic field strength of the j'th ESR line.

Note that the fact that an ESR spectrum belonging to an exchange reaction appears as a single line does not always imply that the fast limit is reached. Such systems may still be in the intermediate region and equation (5) does not hold. In an effort to decide if a given system is indeed exhibiting fast exchange, the following relation may be used [1].

$$Z = \frac{\sqrt{3}}{2}\cdot\frac{\left(\Delta B_{pp} - \Delta B_{pp}^{o}\right)}{\sqrt{\nabla_2}} \le 0{,}2 \tag{7}$$

That is, if $Z \le 0.2$ the system may safely be considered to be in the fast exchange region.

In the intermediate exchange region, the pseudo-first order rate constant, $k = \tau^{-1} = k_{obs}$[A], can been extracted from the experimental spectra by means of density matrix simulations of the dynamically broadened line shapes [2]. Assuming a weakly coupled spin system undergoing degenerate electron exchange in the high temperature limit and a relaxation superoperator diagonal in the subspace of induced transitions, *i.e.* neglecting cross relaxations, the evolution of the relevant terms of the spin density operator in the rotating frame, σ, is governed by:

$$\frac{\partial \sigma_{\beta\{\nu\},\alpha\{\nu\}}}{\partial t} = \left[i\left(\omega_{\alpha\{\nu\},\beta\{\nu\}} - \omega\right) - R_{\beta\{\nu\},\alpha\{\nu\}} - \frac{1}{\tau}\right]\sigma_{\beta\{\nu\},\alpha\{\nu\}} + \frac{2}{N\tau}\sum_{\nu' \neq \nu} \sigma_{\beta\{\nu'\},\alpha\{\nu'\}} + \frac{i\omega_{1,e}\omega_e}{2k_B TN}, \tag{8}$$

where $\{\nu\}$ denotes the set of quantum numbers describing the nuclear spin states and N the dimensionality of the Hilbert space [3]. $R_{\beta\{\nu\}\alpha\{\nu\}}$ is the element of the relaxation matrix corresponding to the induced transition and $\omega_{\alpha\{\nu\},\beta\{\nu\}} = \omega_{\alpha\{\nu\}} - \omega_{\beta\{\nu\}} = (E_{\alpha\{\nu\}} - E_{\beta\{\nu\}})/\hbar$. The absorption signal is obtained from the expectation value of the out of phase magnetization assuming steady state conditions, *i.e.*

$$Y' = Tr\left(\hat{S}_y \hat{\sigma}\right) \propto \mathrm{Im}\frac{-i\sum_k \omega_k n_k F_k}{1 + \frac{2}{N\tau}\sum_k n_k F_k} \tag{9}$$

where the sum now runs over all completely equivalent spin packets of degeneracy n_k and resonance frequency ω_k. N equals the sum over all n_k and τ denotes the average lifetime of the nuclear spin configurations, *i.e.* $\tau^{-1} = k = k_{obs}$ [A]. Furthermore, F_k is defined by $F_k^{-1} = \mathrm{i}(\omega_k - \omega) - T_{2,k}^{-1} - \tau^{-1}$, with $T_{2,k}$ denoting the transversal relaxation time for spin packet k and ω the microwave irradiation frequency, respectively.

Equation (9) has been implemented in Matlab and Fortran 95. Local (trusted region Newton, Simplex) as well as global (Lipschitz, adaptive simulated annealing) optimization algorithms have been employed to fit the experimental spectra. Field modulation effects (100 kHz) have been accounted for by using pseudo-modulation as introduced by Hyde [4].

1.2. Experimental considerations

To obtain the best possible results from ESR line broadening investigations, a certain amount of experimental diligence is required. It may seem superfluous to mention this here, but as it is said: 'God is in the detail'. Albeit information on this subject is ample in literature [5, 6], some key points shall be reiterated.

Any spectrometer setting that might influence the line shape, e.g. modulation amplitude or microwave power, should remain unchanged throughout a series of measurements. Temperature control can be very advantageous as a means of reducing the experimental error. The reason why can be illustrated in the following example: Assuming an Arrhenius-

like behaviour with an activation energy of 15 kJ mol^{-1}, a deviation of the temperature by 1 K around 298K corresponds to a change in rate constant of approximately 2%.

Other things that are often overlooked are the position of the sample in the ESR resonator as well as the so-called filling factor. These are particularly important when working with lossy solvents, as the effective microwave power felt by the paramagnetic species, often expressed by the Q factor, is strongly dependent on the amount of solvent used [7].

Finally, a few remarks on the design of the experiment: In the case of self-exchange, the concentration of the radical is kept constant while varying that of the diamagnetic compound. It is advisable to keep the concentration of the radical low in order to avoid effects from spin exchange, especially when interested in temperature or pressure effects. Often radical concentrations of around 10^{-4} mol l^{-1} are used, whereas the concentration of the diamagnetic compound preferably spans several orders of magnitude. Paramagnetic exchange is treated analogously.

1.3. Experimental techniques in pressure dependent ESR-measurement

Several commercially available temperature-control units exist for magnetic resonance spectroscopic measurements, ranging from liquid helium to very high (1100°C) temperatures.

In contrast units for pressure dependent experiments must be constructed by the experimentalist themselves.[1] Fortunately, several excellent books are published on high-pressure techniques covering a great variety of experimental measurements and different spectroscopies [8, 9]. To our knowledge no special review concerning ESR-spectroscopy under high pressure exists, but several articles describing high-pressure cells for NMR- and ESR-spectroscopy. Many experimental details developed for high-pressure NMR-cells can be adapted for ESR-spectroscopy often in simpler versions [10-13]. Several publications deal with high-pressure magnetic resonance cells for solid state investigations [14-21]. Even high-pressure cells for ENDOR-studies [22], for K-band (23 GHz) ESR-cavities [23] and for helix ESR-resonators [24, 25] are reported.

Since this article focuses on liquid samples, only details of pressure-dependent papers will be considered here. A short overview on different investigations is given.

A detailed description for a high-pressure ESR-cell up to 900 MPa using quartz glass capillaries is reported by Yamamoto et al. [26]. An apparatus for studying ESR of fluids in a flow cell under high pressure and high temperature is described by Livingston and Zeldes [27]. Measurements up to 12.4 MPa and 500°C are used to study polymerization and catalysis [28]. Even a combination of high-pressure and rapid mixing stopped-flow techniques is realized [29]. A simple system for measurements in water up to 60 MPa is described by Cannistraro [30].

[1] The only commercial high-pressure ESR-cell was offered by: High Research Center, Unipress Equipment Division, Warszawa, Poland.

Important Russian contributions to high pressure ESR-cells for solid state investigations appeared in the early 1970s [31, 32].

An early contribution published by Maki et al. describes the temperature- and pressure dependence on the spin exchange kinetics and the change in ESR-line widths of the di-tert-butyl nitroxide (DTBN) radical in various solvents [33, 34]. Also the nitrogen ESR-hyperfine splitting, a^N, of DTBN was measured in solution as a function of the pressure [35]. Freed et al. looked at the pressure dependence of ordering and spin relaxation in liquid crystals [36].

Solvated electrons and their reaction behavior under high pressure is published by Schindewolf et al. together with experimental details of the high-pressure cell [37]. The line width of vanadyl acetylacetonate was investigated in a number of non-hydrogen bonded solvent together with its anisotropic interactions [38]. Biochemical spin label studies in solution up to 300 MPa are reported together with a detailed cell construction [39]. Well studied kinetic phenomena like the cation migration within p-quinone radical anions have been studied up to 63.7 MPa. Activation volumes for different cations are reported [40]. Even CIDEP-experiments were performed to get information on the pressure dependence of the spin-lattice relaxation time [41].

Several papers deal with investigations on various nitroxides. The pressure of the spin exchange rate constants of 2,2,6,6-tetramethyl-4-oxo-1-piperidinoxyl (4-oxo-TEMPO) was measured in different solvents, both unpoar and polar. Up to 58.8 MPa the rate constants vary between 10^9 – 10^{10} $M^{-1}s^{-1}$ [42]. Experimental and calculated activation volumes are compared for these reactions [43]. These investigations were extended to DTBN and 2,2,6,6-tetramethyl-1-piperidinoxyl radical (TEMPO) [44] and finally to 4-Hydroxy-TEMPO, 4-Amino-TEMPO, Carboxy-PROXYL, Carbamoyl-PROXYL, 5-DOXYL and 10-DOXYL. From the rate constants and the activation volumes obtained the authors were able to calculate the corresponding exchange integral J for each reaction [45]. The pressure dependence of the inclusion equilibrium of diphenylmethyl t-butyl nitroxide and DTBN with β- and γ-cyclodextrins were studied in detail [46,47]. The effect of pressure and the solvent dependence of the intramolecular spin-exchange of biradicals with two nitroxide fragments linked by a long flexible chain were obtained from ESR.-lifetimes studies of the radical fragments inside and outside the cage. The nearly cyclic conformation in the cage is reported as the favorable one in solution [48]. A short review in Japanese appeared on the spin exchange kinetics of nitroxides [49]. Applications of the spin-label technique at high pressures is reported up to the high pressure of 700 MPa [50]. Recently Hubbell et al. [51] published the design of a high-pressure cell using polytetrafluoroethylene (PTFE) coating fused silica capillary tubes up to 400 MPa. Bundles of these capillaries are placed inside an ESR-cavity. This cell is adapted from an NMR-cell designed by Yonker et al. [52].

Another recent high pressure setup was used to investigate electron self-exchange reactions [53]. The experimental arrangement used by the authors is illustrated in figure 2. A hand-driven high-pressure pump is connected with the medium exchanger, separating sample solution and pressure medium, using ethylene glycol as pressure medium. The sample-side of the system can evacuated for sample changing and cleaning.

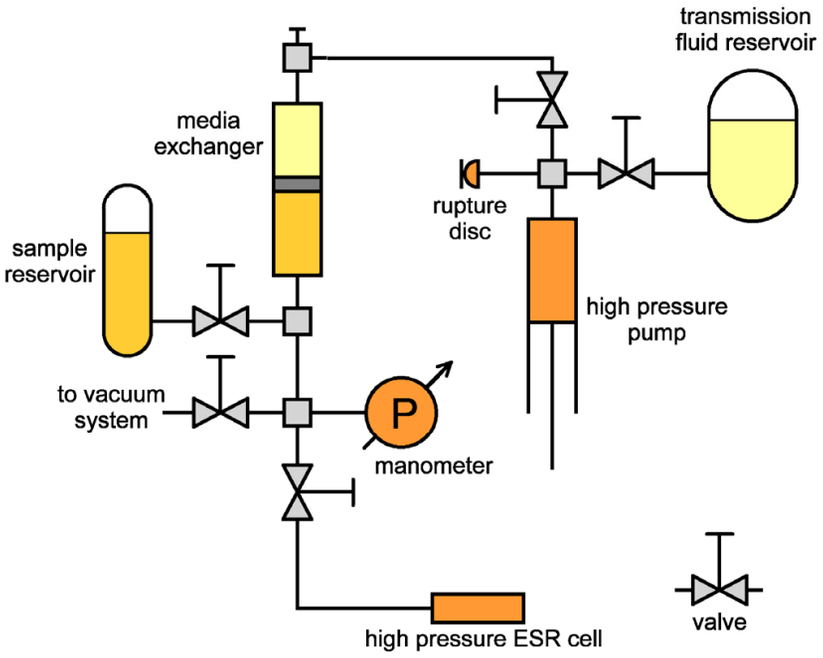

Figure 2. Diagram of a typical arrangement for experiments at elevated pressures [53].

2. Electron self-exchange reactions

The ESR line broadening method was first used by Ward and Weissman [54] in 1957 when they investigated the self-exchange reaction between naphthalene and its radical anion. In the following decade, Weissman continued his work, adding information on further systems as well as refining the theoretical treatment of the experiment [55]. Other important contributors were Miller and Adams [56], who investigated several systems using electrochemically generated radicals. These authors were among the first to use this technique to make a comparison between homogeneous and heterogeneous electron transfer according to the Marcus Theory [57]. Since then, numerous other authors have made their contributions, covering many aspects of the self-exchange reaction, including temperature dependencies and effects from counter ions and solvent.

2.1. Theory

The theoretical aspects of electron transfer in solution originate in the 1950s with the pioneering work of Marcus [58-60], who offered a description of the energetics of both the self-exchange and the general reaction. Since then the theory has greatly evolved [61-63], as shall be discussed in the theoretical part of this chapter, where especially solvent (dynamic) effects are of interest.

In general, self-exchange denotes the one-electron transfer between the partners of a redox couple, which results in no net chemical reaction. The mechanism is shown in figure 3, using a radical anion, $A^{\bullet -}$, and its neutral parent compound, A.

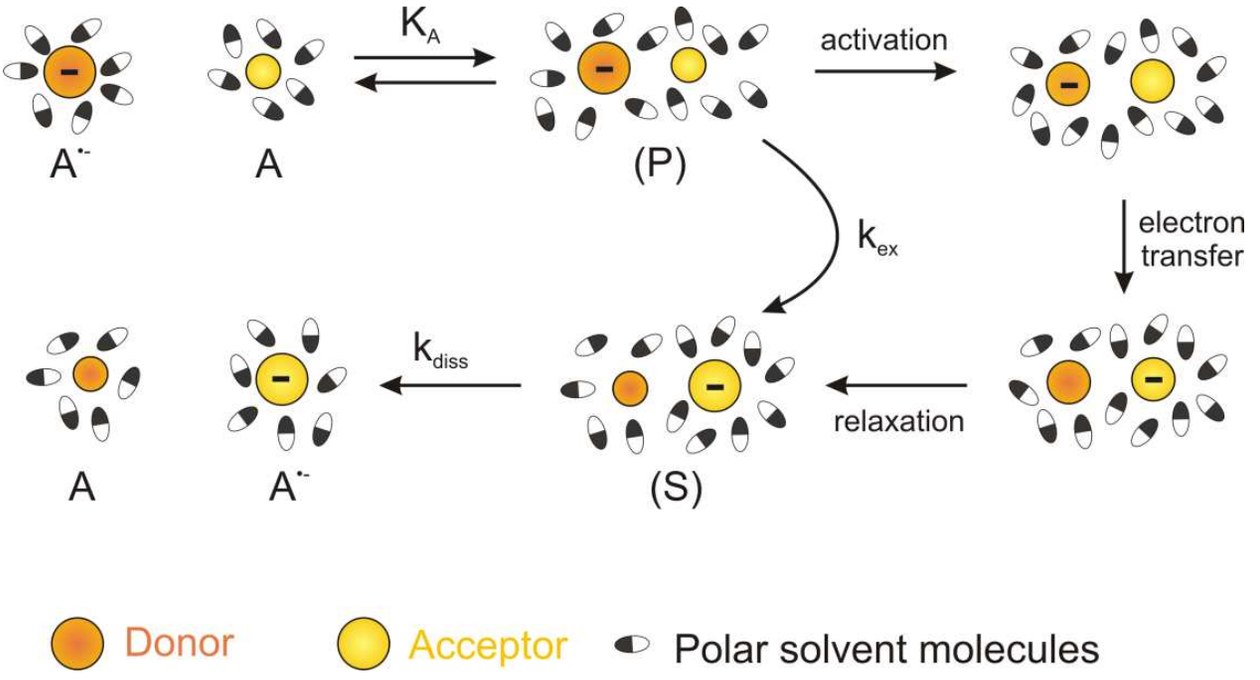

Figure 3. The reaction mechanism of an electron transfer reaction.

The bimolecular electron transfer rate constant, $k_{et} = K_A k_{ex}$, is expressed as

$$k_{et} = K_A \kappa_{el} \nu_n \exp\left(\frac{-\Delta G^*}{RT}\right) \tag{10}$$

Here, $K_A = 4\pi N_A \sigma^2 \delta\sigma$ is the formation constant of the precursor complex, which in turn is expressed by Avogadro's number, N_A, the reaction distance σ and the reaction zone thickness $\delta\sigma$. Further in equation (10), κ_{el} is the electronic transmission coefficient, υ_n the nuclear collision frequency and ΔG^* energy of activation according to Marcus.

Figure 4 depicts the energy surfaces of precursor and successor complexes, simplified in a two-dimensional representation of energy as a parabolic function of reaction coordinate. From this it is possible to express the activation energy as $\Delta G^* = \lambda/4 - V_{PS}$, using the reorganization energy, λ, and the resonance splitting energy, V_{PS}.

Strictly speaking, the Marcus equation only applies to the precursor and successor complexes. In most cases, however, no information is available about these and therefore it is desirable to express the Marcus equation in terms of the reactants, A and $A^{\bullet-}$. In the case where both reactants have nonzero charges, zA and zD, a work term, W, accounting for the Coulombic work needed to bring the reactants together must be included,

$$W = \frac{z_A z_D e_0^2}{4\pi\varepsilon_0\varepsilon_S\sigma} \tag{11}$$

with e_0 representing the electronic charge, ε_S the dielectric constant of the medium, σ the reaction distance.

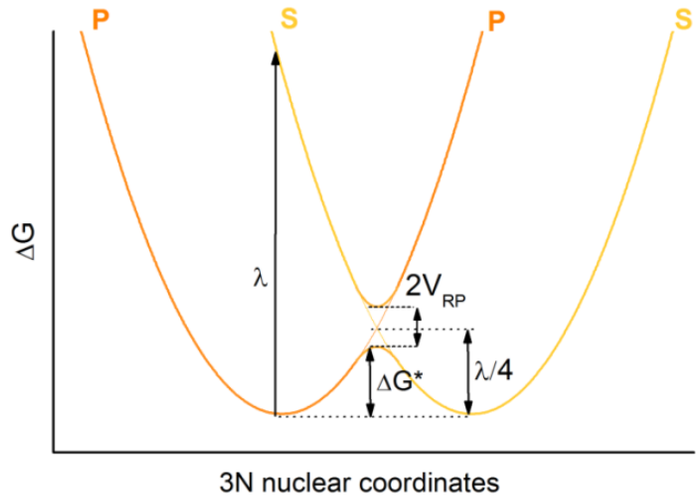

Figure 4. Energy diagram of the self-exchange reaction

Resulting, the expression of the Marcus equation takes the following form:

$$\Delta G^{*} = W + \frac{\lambda}{4} - V_{PS} \tag{12}$$

The reorganization energy, λ, is an energetic measure of the changes the reactants and their surroundings undergo as the reaction proceeds.

Commonly, the reorganization energy is split into two contributions, the inner and outer reorganization energies, λ_i and λ_o , respectively.

$$\lambda = \lambda_i + \lambda_o \tag{13}$$

λ_i, takes into account the changes in bond lengths and/or angles in the reactants undergoing electron transfer. In the classic high temperature limit, where all vibrational frequencies fulfil $\nu_n \ll k_B T/h$ (not confusing ν_n with the collision frequency), λ_i is given by:

$$\lambda_i^{\infty} = \sum_j \frac{f_R^j \cdot f_P^j}{f_R^j + f_P^j} \left(\Delta q_j\right)^2 \tag{14}$$

Here, $f_{R,P}^j$ is the force constant of bond j, either in the reactants, R, or the products P, and Δq_j expresses the change in length of bond j. Unfortunately this approach has certain drawbacks when organic redox couples are considered, as it becomes increasingly difficult to find all important vibrations contributing to the reaction coordinate. The situation worsens further as the high temperature approximation is not always valid, meaning that corrections for quantum-mechanical tunnelling should be included. This was pointed out by Holstein [64], and used by several other authors like Bixon and Jortner [61, 65], and Sutin [66] yielding an equation of the following type:

$$\lambda_i(T) = \lambda_i^{\infty} \frac{4k_B T}{h\bar{\nu}} \tanh\left(\frac{h\bar{\nu}}{4k_B T}\right) \tag{15}$$

where $\bar{\nu}$ =5·10[13] s[-1] is used as the mean vibration frequency for organic redox couples.

A method of calculating λ_i^{∞} , without explicitly knowing the changes in bond-lengths and force constants, has been published by Nelsen *et al.* [67,68], needing the energies of four distinct points on the energy surfaces of products and reactants. By calculating the energies of the reactants in their most stable geometrical configuration, as well as in the most stable configuration of the products, together with analogous calculations for the products, λ_i^{∞} may be obtained.

The outer reorganization energy, λ_o, which is sometimes also referred to as the solvent reorganization energy, describes the change in polarization of the solvent molecule surrounding the activated complex. Marcus showed that the outer reorganization energy may be expressed as in equation (16), using a simple dielectric continuum model and assuming that the reactants are spherical.

$$\lambda_o = \frac{e_0^2 N_A}{4\pi\varepsilon_0} g(r,\sigma)\cdot\gamma \tag{16}$$

Here, apart from the permittivity of vacuum, ε_0, new parameters are the function g(r,σ) which depends on the geometry of the transition state, and γ, the so-called Pekar factor, which depends on the dielectric properties of the solvent.

In its simplest form, assuming $r_A=r_{A^{\bullet-}}=r$, using spherical models of the reactants, g(r, σ) is given by:

$$g(r,\sigma) = \frac{1}{r} - \frac{1}{\sigma} \tag{17}$$

Often the reaction distance, σ, is assumed to be that of close contact, here being twice the radius of the reactants: σ=2r. For organic molecules, this approach is often too simple, as the geometry can no longer be assumed to be spherical. If, in stead, an ellipsoidal model is used, r is replaced by the mean elliptic radius, $\bar{r}$:

$$\bar{r} \approx \frac{\left(a^2-c^2\right)^{1/2}}{F(\varphi,\alpha)} \tag{18}$$

with the elliptic semi axes fulfilling a > b > c and F(ϕ,α) being elliptic integrals of the first kind, using $\varphi = \arcsin\left[\left(a^2-c^2\right)^{1/2}/a\right]$ and $\alpha = \arcsin\left[\left(a^2-b^2\right)/\left(a^2-c^2\right)\right]^{1/2}$ [69]. A good approximation has been found to be: $\bar{r} = \frac{1}{3}(a+b+c)$.

Another approach has been suggested by Compton and co-workers [70, 71] who, instead of calculated radii, use experimentally determined hydrodynamic radii.

As intermolecular orientation becomes more difficult to describe, the reaction distance may also be modified using the ellipsoid model [72, 73], replacing σ, with the apparent reaction distance, σ′:

$$\frac{1}{\sigma'} = \frac{1}{\sigma}\left[1 + \frac{2c^2 - a^2 - b^2}{3\sigma^2} + \frac{abc}{\sigma^3} + \frac{4\left(8c^4 + 3\left(a^4 + b^4\right) - 8c^2\left(a^2 + b^2\right) + 2a^2b^2\right)}{15\sigma^4}\right] \tag{19}$$

The second contribution to the reorganization energy, the solvent dependent Pekar factor, γ, in turn, is given by

$$\gamma = \frac{1}{\varepsilon_\infty} - \frac{1}{\varepsilon_S} \tag{20}$$

where ε_S and ε_∞ are the static and optical dielectric constants, respectively. Unfortunately, reliable experimental values of ε_∞, can be very hard to come by, so it has become common practice to use the refractive index, n_D, in an approximation: $\varepsilon_\infty = n_D^2$.

Apart from the obvious solvent dependence of the reorganization energy, the rate constant of an electron transfer reaction may also be influenced by the solvent in terms of the nuclear frequency factor, ν_n.

Originally, Marcus expressed ν_n using a simple gas-phase collision model [74], yielding equation (21),

$$\nu_n = \sigma^2 N_A \left(\frac{16\pi RT}{M}\right)^{1/2} \tag{21}$$

with the only new parameter being the molar mass, M.

The solvent dependence is introduced by taking the formation of the precursor complex into account, expressing the total frequency factor as combination of those of the solvent, ν_o and the reactants, ν_i, weighted by the respective reorganization energies.

$$\nu_n = \left(\frac{\nu_i^2 \lambda_i + \nu_o^2 \lambda_o}{\lambda}\right)^{1/2} \tag{22}$$

Equation (22) is valid only for rapid dielectric relaxation in the solvent. For slow dielectric relaxation, the longitudinal relaxation time of the solvent, τ_L, must be included as the solvent relaxation now happens on the same time scale as the reaction. This observation was first made by Kramers [75], who spoke of a solvent dynamic effect or solvent friction, and the theory was later expanded by authors like Zusman [76, 77], Jortner and Rips [61, 78, 79], Marcus and Sumi [63] as well as several others.

The longitudinal relaxation time may be determined from the usual dielectric parameters of the solvent [80],

$$\tau_L = \frac{\varepsilon_\infty}{\varepsilon_S}\tau_D \tag{23}$$

with, τ_D being the Debye relaxation time, which itself may be expressed using the molar volume, V_M, and the viscosity, η, of the solvent:

$$\tau_D = \frac{3V_M\eta}{RT} \tag{24}$$

Assuming that $\lambda_i << \lambda_o$, the nuclear frequency factor then becomes:

$$\nu_n = \frac{1}{\tau_L}\left(\frac{\lambda_o}{4\pi RT}\right)^{1/2} \tag{25}$$

So far it has been supposed that the electron transfer reaction was adiabatic, assuming the transmission factor, κ_{el}, to be unity. This applies to all reactions studied in this work, but for completeness, the expression valid in the case of diabatic electron transfer [69, 76, 81, 82] is given here:

$$\kappa_{el}\nu_n = \frac{2\pi V^2}{\hbar N_A\left(4\pi\lambda_o RT\right)^{1/2}} \tag{26}$$

It is now possible to discern the nature of the electron transfer by the use of simple mathematical treatment, calculating the experimental value, $(\kappa_{el}\nu_n)_{obs}$ as suggested by Weaver [83, 84],

$$\left(\kappa_{el}\nu_n\right)_{obs} = k_{et,obs}K_A^{-1}\exp\left(\frac{\Delta G^*_{calc}}{RT}\right) \tag{27}$$

where $k_{et,obs}$ is the experimentally determined rate constant and ΔG^*_{calc} the activation energy calculated using equation (12). Double logarithmic plots determine the type of electron transfer observed. In the general Marcus case, a constant value of ln $(\kappa_{el}\nu_n)_{obs}$ is expected, whereas the diabatic and adiabatic cases both produce straight lines with slopes of unity when plotted against ln $(\gamma^{-1/2})$ or ln $(\gamma^{1/2}\tau_L^{-1})$, respectively.

It is well-known that, k_{ex} depends on temperature and pressure. The temperature dependence is seen directly in equation (28), but also in the dependencies of the activation energy, via γ, and that of the nuclear frequency factor.

$$k_{ex}\left(p,T\right) = \kappa_{el}\nu_n\left(p,T\right)\exp\left(\frac{-\Delta G^*\left(p,T\right)}{RT}\right) \tag{28}$$

The temperature dependence of ν_n is often neglected in the general Marcus case and that exhibiting diabatic solvent dynamics. However, when dealing with adiabatic solvent

dynamics, the temperature dependence must be included, due to the fact that τ_L may vary strongly with temperature, according on the solvent in question. In some cases even, this variation may be of more than an order of magnitude, as in the case of propylene carbonate, where τ_L is 42.6 ps at 228 K and 2.6 ps at 308 K [85].

The pressure dependence is usually expressed using the activation volume, $\Delta^{\ddagger}V$:

$$\Delta^{\ddagger}V = -RT\left(\frac{\partial \ln k_{ex}}{\partial P}\right)_T \tag{29}$$

In terms of transition state theory, the activation volume may be expressed using the volume of the transition state, $^{\ddagger}V$ and the molar volumes of the reactants, V_A and $V_{A^{\bullet-}}$, cf. equation (30),

$$\Delta^{\ddagger}V = {}^{\ddagger}V - \left(V_A + V_{A^{\bullet-}}\right) \tag{30}$$

and thus represents the changes in volume involved in the electron transfer process. This is also seen in figure 5, where the volume profile of a reaction with a positive volume of activation is shown.

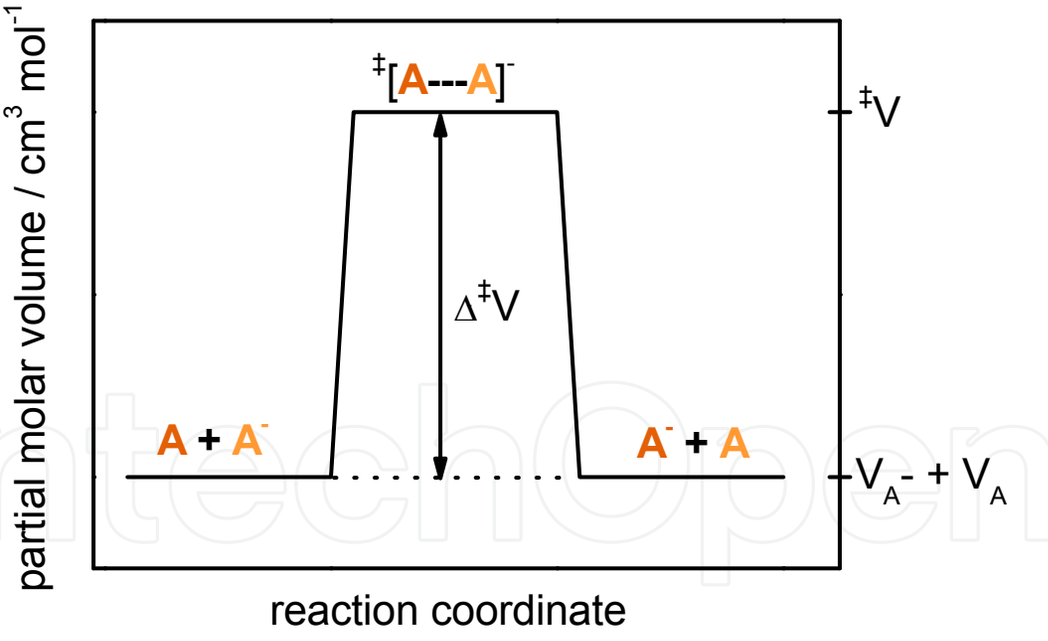

Figure 5. Volume profile of an electron transfer reaction

Generally, one may also define a reaction volume, $\Delta_r V$, as the difference in the volumes of products and reactants, but for self-exchange reactions, this becomes zero.

As in the case of ΔG^*, one may seek to describe the activation volume by separating the various contributions. This has been discussed in great detail by Swaddle [10, 86-88], who

derived expressions of the contributions from inner and outer reorganization, $\Delta^{\ddagger}V_i$ and $\Delta^{\ddagger}V_o$, Coulombic work, $\Delta^{\ddagger}V_{Coulomb}$, Debye-Hückel effects, $\Delta^{\ddagger}V_{DH}$, solvent dynamics, $\Delta^{\ddagger}V_{SD}$, and finally a contribution from the non-Coulombic part of the precursor complex formation constant, $\Delta^{\ddagger}V_{PREC}$. Summing up the different parts, the volume of activation of the self-exchange reaction is calculated as expressed in equation (31).

$$\Delta^{\ddagger}V_{calc} = \Delta^{\ddagger}V_i + \Delta^{\ddagger}V_o + \Delta^{\ddagger}V_{Coulomb} + \Delta^{\ddagger}V_{DH} + \Delta^{\ddagger}V_{SD} + \Delta^{\ddagger}V_{PREC} \tag{31}$$

Each of these contributions is treated separately by differentiation of the respective energetic expressions.

The contribution to the activation volume, arising from inner reorganization is usually neglected, as the increase in volume of the acceptor almost cancels the decrease in volume of the donor. Stranks [89] showed that in most cases, a value of 0.6 $cm^3\ mol^{-1}$ may be taken for $\Delta^{\ddagger}V_i$, which is usually close to the experimental uncertainty of $\Delta^{\ddagger}V$. The contribution from $\Delta^{\ddagger}V_{PREC}$ is also expected to be small since both σ and $\delta\sigma$ are practically pressure independent [88].

Taking the Marcus expression for the outer reorganization energy, λ_o, and assuming that only the Pekar factor, γ, is pressure dependent, and additionally taking into account compression of the solvent, $\Delta^{\ddagger}V_o$, must be given as shown in equation (32), remembering that λ_o only contributes with a quarter of its value to the activation energy.

$$\Delta^{\ddagger}V_o = \frac{1}{4}\left(\frac{\partial\lambda_o}{\partial P}\right)_T = \frac{e_0^2 N_A}{16\pi\varepsilon_0}\left[\left(\frac{1}{r}-\frac{1}{\sigma}\right)\left(\frac{\partial\gamma}{\partial P}\right)_T - \gamma\frac{\beta}{3\sigma}\right] \tag{32}$$

The Pekar factor is approximated as $\gamma = n^{-2} - \varepsilon_S^{-1}$ using the refractive index, n, and static dielectric constant, ε_S, of the solvent and the isothermal compressibility of the solvent, β, is defined via its density, ϱ, as $\beta = \rho^{-1}\left(\frac{\partial\rho}{\partial P}\right)_T$.

By simple differentiation of the work term given in equation (11), the Coulombic contribution to the activation volume is found.

$$\Delta^{\ddagger}V_{Coulomb} = \frac{z_A z_D e_0^2 N_A}{4\pi\varepsilon_0\sigma}\left(\frac{\partial\varepsilon_s^{-1}}{\partial P}\right)_T \tag{33}$$

The expression for $\Delta^{\ddagger}V_{DH}$ is derived from the extended Debye-Hückel theory, and takes the following, rather cumbersome, form:

$$\Delta^{\ddagger}V_{DH} = \frac{RTz_A z_D C I^{1/2}}{\left(1+BaI^{1/2}\right)^2}\left[\left(\frac{\partial\ln\varepsilon}{\partial P}\right)_T\left(3+2BaI^{1/2}\right)-\beta\right] \tag{34}$$

with a, B; and C being the Debye-Hückel constants and I the ionic strength.

These two contributions are of opposite sign and usually, for values of I between 0.1 and 0.5, tend to cancel each other quite conveniently [86, 87]. In the case where neutral molecules are involved, as it is in the experimental part of this work, both $\Delta^{\ddagger}V_{Coulomb}$ and $\Delta^{\ddagger}V_{DH}$ are zero.

Recalling that the solvent dynamic effect is manifested in the pre-exponential term of the Arrhenius equation, the following definition offers itself readily:

$$\Delta^{\ddagger}V_{SD} = RT\left(\frac{\partial \ln\left(\kappa_{el}\nu_n\right)}{\partial P}\right)_T \tag{35}$$

This may then be further elaborated in the cases of diabatic and adiabatic solvent dynamics, as shown shortly. Note that even in the general Marcus case, with $\kappa_{el}\nu_n$ depending on σ, a slight pressure dependence is expected, but as argued earlier, this may be neglected. However, due to the logarithmic form of equation (35), it is now considerably simpler to describe the influence of σ, as all constants in equation (21) are conveniently eliminated. Assuming that σ compresses approximately as the solvent, i.e. $\sigma \propto \rho^{-1/3}$, the contribution to the activation volume should be obtainable with relative ease.

In the diabatic case given in equation (36), $\Delta^{\ddagger}V_{SD}$ becomes:

$$\Delta^{\ddagger}V_{SD} = RT\left(\frac{\partial}{\partial P}\left(\ln\frac{2\pi V^2}{\hbar N_A\left(4\pi\lambda_o RT\right)^{1/2}}\right)\right)_T = -\frac{RT}{2}\left(\frac{\partial \ln\gamma}{\partial P}\right)_T \tag{36}$$

with all pressure independent quantities eliminated as above. In cases of strong diabaticity, where a noticeable dependence of k_{ex} on σ is expected, one must include the pressure dependence of V_{PS}, which follows the principle discussed in the Marcus case, and shall not be further elaborated here.

For electron transfer exhibiting adiabatic solvent dynamic behaviour, the situation becomes slightly more complicated, as now also the longitudinal relaxation time contributes to $\Delta^{\ddagger}V_{SD}$.

$$\Delta^{\ddagger}V_{SD} = RT\left(\frac{\partial}{\partial P}\left(\ln\frac{1}{\tau_L}\left(\frac{\lambda_o}{4\pi RT}\right)^{1/2}\right)\right)_T = RT\left[\frac{1}{2}\left(\frac{\partial \ln\gamma}{\partial P}\right)_T - \left(\frac{\partial \ln\tau_L}{\partial P}\right)_T\right] \tag{37}$$

Returning to electron self-exchange reactions, where the activation volume consists of the five parts, which have just been introduced, by far the greatest contribution is expected from $\Delta^{\ddagger}V_o$. As already mentioned, $\Delta^{\ddagger}V_{Coulomb}$ and $\Delta^{\ddagger}V_{DH}$ tend to cancel each other, or even vanish when an uncharged molecule is reacting, and $\Delta^{\ddagger}V_i$ is generally negligible. Consequently, one may write:

$$\Delta^{\ddagger}V = \Delta^{\ddagger}V_o + \Delta^{\ddagger}V_{SD} \tag{38}$$

In other words, the activation volume may be interpreted as owing to a term described by the energy barrier crossed during the reaction, $\Delta^{\ddagger}V_o$, and a term linked to the actual crossing

of the barrier, $\Delta^{\ddagger}V_{SD}$. Even here, the contribution from the pre-exponential factor is unimportant in the general Marcus case and in that of diabatic solvent dynamics, leaving only the adiabatic case with an appreciable contribution.

Typical values of $\Delta^{\ddagger}V$ are found to be in the range of -30 to +30 $cm^3\ mol^{-1}$ [10], corresponding to a retardation or acceleration of the reaction of about a factor of 4 at 100 MPa as compared to ambient pressure (0,1 MPa).

2.2. Experimental

As mentioned above, much work has been done using ESR line broadening experiments to study self-exchange reactions; however, only in surprisingly few cases nitroxides have been involved. Nitroxides are readily oxidized [90-92] to form the diamagnetic compound needed in the self exchange with the neutral radical. In most cases, the ESR spectra remain within the slow exchange region due to the relatively large nitrogen hyperfine splitting constant. The reported results have dealt with the self-exchange of various nitroxide couples in acetonitrile [93] as well as of that of TEMPO with its oxidized counterpart in several different solvents [94]. For the latter couple, the temperature dependence of the exchange reaction has also been investigated [95].

Some typical spectra are shown in figure 6 together with the accompanying plot to determine k_{obs}. Subsequently, the electron transfer rate constant, k_{et}, can be obtained applying a correction for diffusion as shown in equation (39).

$$\frac{1}{k_{obs}} = \frac{1}{k_{et}} + \frac{2}{k_d} \tag{39}$$

The factor of two seen on the last term of equation (39), as opposed to that of one which is seen in more general reactions, is due to the nature of the self-exchange reaction.

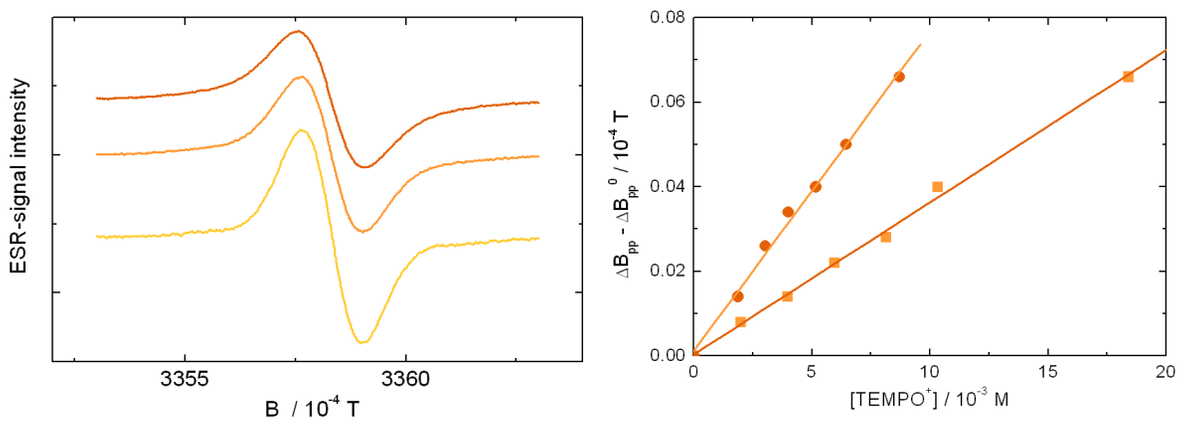

Figure 6. Left: Central lines of the ESR spectra of TEMPO in acetonitrile. Concentrations of $TEMPO^+\ Cl^-$ were 0 mM (bottom) 8 mM (middle) and 18 mM (top). Right: Concentration dependence of the change in peak-to-peak line width in water (squares) and propylene carbonate (circles).

The experimental results of references [94] and [95] serve as a good example of how ESR line broadening experiments can be utilized to study solvent effects on electron transfer.

Table 1 presents the electron transfer rate determined as given above, together with relevant solvent properties and the quantities needed to investigate the presence of a solvent effect.

Solvent	k_{et} / 10^8 l mol^{-1} s^{-1}	k_{diff} / 10^8 l mol^{-1} s^{-1}	γ	τ_L / ps	ΔG^*_{calc} / kJ mol^{-1}	$(\kappa_{el}\nu_n)_{obs}$ / 10^{14}s^{-1}
Acetonitrile [94]	2.6±0.2	190	0.527 [96]	0.21 [96]	35	20
Benzonitrile [94]	2.2±0.1	52.4	0.389 [85]	5.75 [85]	27,2	0.67
Deuterium Oxide [94]	1.4±0.1	51.9	0.554 [97]	0.593 [97]	36.5	20
Methanol [95]	0.50±0.05	109	0.537 [98]	9.36 [98]	35.5	4.7
Propylene Carbonate [94]	2.1±0.2	23.5	0.480 [85]	3.27 [85]	32.3	5.2
Tetrahydrofuran [94]	5.0±0.3	114	0.37 [69]	1.7 [69]	26	1.1
Water [94]	0.82±0.07	64.8	0.550 [99]	0.812 [99]	36.3	10
Water [95]	0.72±0.06	64.8	0.550 [99]	0,812 [99]	36.3	8.5

Numbers in brackets correspond to the relevant reference.

Table 1. Self-exchange rate constants TEMPO/TEMPO$^+$ in pure solvents at 293K

The values of ΔG^*_{calc} listed in table 1 were determined using a λ_i of 33 kJ mol^{-1} and λ_o of 191 $\times\gamma$ kJ mol^{-1}. Both values were calculated [95] as shown above, and have been confirmed experimentally by other authors [100].

Values of $(\kappa_{el}\nu_n)_{obs}$ were obtained using equation (27), and as it is clearly not solvent independent, the general Marcus type of electron transfer is immediately ruled out and the existence of a solvent dynamic effect is successfully demonstrated. The nature of this is shown in figure 7 where the appropriate double logarithmic plots are given.

From figure 7 it can clearly be seen that the presence of a diabatic solvent effect can be excluded, since a line with a slope of unity would be needed to confirm the corresponding assumption. The line shown in the right hand plot of the figure has been fixed to this slope and thereby shows that an adiabatic solvent effect is likely in the case of self-exchange in the TEMPO/TEMPO$^+$ system.

Since the literature values of the dielectric properties of the solvents are often subject to large uncertainties error bars have been introduced in each diagram to illustrate the range of

values corresponding to errors of 10% in each γ and τ_L. In the case of the former an error of such magnitude is highly unexpected, but for the latter, 10% might even be considered conservative in some cases.

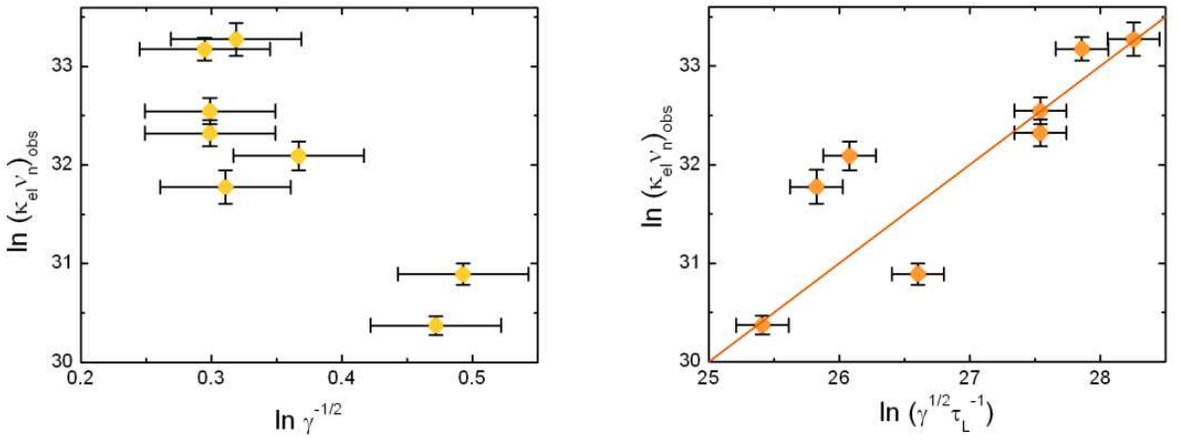

Figure 7. Diagrams assuming diabatic (left) and adiabatic (right) solvent dynamic effects. X-axis error bars correspond to a 10% error on each γ and τ_L. The line has a fixed slope of one.

In fact, regarding the longitudinal relaxation time needed in the calculations concerning the adiabatic case a few remarks must be made. In many solvents and electrolyte solutions, high precision experiments have indicated the existence of several relaxation pathways in the solvent. Usually it is assumed that only the slowest of the relaxation processes will influence the electron transfer reaction [76, 101] and the τ_L to be used in investigations of solvent dynamic effects, is thus the largest of the relaxation times:

$$\tau_{iL} = \frac{\varepsilon_{i\infty}}{\varepsilon_{iS}} \tau_{iD} \quad i = 1, 2, \ldots \tag{40}$$

As an example, take methanol [98] which has two relaxations with parameters at 293K: $\varepsilon_S = \varepsilon_{1S} = 32.5$, $\varepsilon_{1\infty} = \varepsilon_{2S} = 5.91$, $\varepsilon_{2\infty} = \varepsilon_\infty = 4.9$ and $\tau_{D1} = 51.49$ ps, $\tau_{D2} = 7.09$ ps, leading to $\tau_{L1} = 9.36$ ps and $\tau_{L2} = 5.88$ ps. For comparison, both older and newer works [102-105] report only a single relaxation process for methanol, resulting in a τ_L which ranges from 4.58 ps to 10.6 ps. The reason that these latter experiments have only detected one relaxation time is, that they have been conducted using a relatively narrow frequency range and thus a long extrapolation for determination of ε_∞.

Having established that the solvent dynamic effect is adiabatic, a plot of ln ($k_{et}\tau_L\gamma^{-1/2}$) vs. γ allow the calculation of g(r,σ') since,

$$\ln\left(k_{et}\tau_L\gamma^{-\frac{1}{2}}\right) = const - \frac{\lambda_o}{4RT} = const - \frac{e_0^2 g\left(r,\sigma'\right)}{16\pi\varepsilon_0 k_B T}\gamma \tag{41}$$

From the slope of this plot, while taking $r = \bar{r} = 3.11$ Å, the reaction distance becomes $\sigma' = 5.0$ Å, which is in reasonably good agreement with the value of $\sigma' = 5.4$ Å found in the theoretical calculations [94]. The experimental value of σ' corresponds to $K_A = 0.21$ l mol^{-1}.

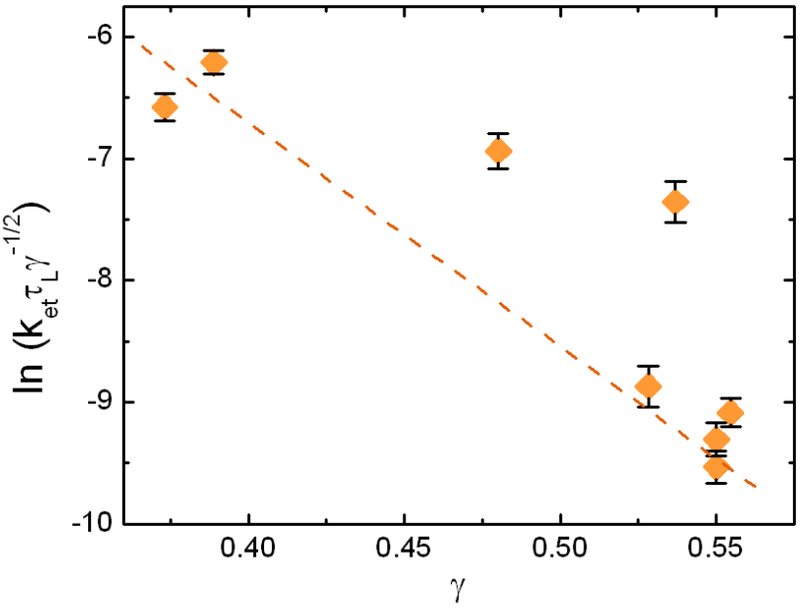

Figure 8. 'Traditional' diagram for illustration of the adiabatic solvent dynamic effect. The slope of the dotted line corresponds to a reaction distance of 5.0 Å.

The listed rate constants were used to determine the activation energy of the reaction in each of the solvents, which, due to the adiabatic solvent dynamics, was done by plotting ln ($k_{et}\tau_L\gamma^{-1/2}T^{1/2}$) vs. T^{-1} as can be seen in table 2. For comparison, the values obtained from common Arrhenius plots (ln k_{et} vs T^{-1}) are also shown. The table also contains the longitudinal relaxation energies of the solvent as well as the quantity ΔH^*_{calc}, which represents a theoretical prediction of the activation enthalpy, taking into account the temperature dependency of the reorganization energy [95].

The concerns regarding the physical properties of solvents become even more pronounced when dealing with temperature dependencies. Once again, the longitudinal relaxation time provides the greatest problem as the relaxation energy, H_L, varies tremendously in literature. Using the example of methanol again, H_L could only be obtained from data using a single relaxation time, whereas for THF no less than four values are reported, ranging from -8.3 kJ mol^{-1} [106] to 11.1 kJ mol^{-1} [107].

Returning to the experimental activation energies and enthalpies, it is seen that the relation $E_a = \Delta H^* + H_L$ is fulfilled within the experimental error, as expected due to the Arrhenius-like temperature dependence of the involved quantities, with any deviations being mainly due to the slight temperature dependence of γ. The results illustrate the importance of knowing whether or not solvent dynamics are present in an electron transfer system before determining the activation parameters. The activation energies from the traditional Arrhenius plots do not correspond to Marcus' ΔG^* due to the involvement of τ_L. To make matters worse, neither does the energy obtained from the plots of ln ($k_{et}\tau_L\gamma^{-1/2}T^{1/2}$) vs. T^{-1},

since both λ_i and λ_o are temperature dependent. For this reason the values in the table have been labeled as enthalpies in order to signify that they correspond to the temperature independent part of ΔG*. Taking the temperature dependence of ΔG* into account, it is possible to reach a theoretical estimate of this enthalpy, ΔH^*_{calc} [95]. As can be seen, for acetonitrile, benzonitrile, tetrahydrofuran and water, good agreement is found between experiment and theory. This is not the case for the three remaining solvents, where large discrepancies are found. Except for propylene carbonate, the main reason for the poor agreement is likely to be the quality of the dielectric data as already discussed.

Solvent	Energy / kJ mol^{-1}			
	E_a [a]	ΔH^* [b]	H_L [c]	ΔH^*_{calc} [d]
Acetonitrile [94]	18.2±0.7	18.1±0.7	1.0 [96]	19
Benzonitrile [94]	23.9±0.7	14.1±0.4	11.0 [85]	15
Deuterium Oxide [94]	15±2	-4.3±0.5	19.0 [97]	25
Methanol [95]	21±2	8.8±0.5	12.8 [102]	31
Propylene Carbonate [94]	13±1	-7±1	20.9 [85]	18
Tetrahydrofuran [94]	6.7±0.8	16.6±0.4	-8.3 [106]	19
Water [94]	6.5±0.2	22.7±0.5	-14.9 [99]	24
Water [95]	6.8±0.1	22.9±0.4	-14.9 [99]	24

[a] Activation energy determined from a traditional Arrhenius plot (ln k_{et} vs. T^{-1})

[b] Activation energy determined assuming adiabatic solvent dynamics (ln $k_{et}\tau_L\gamma^{-1/2}T^{1/2}$ vs. T^{-1})

[c] Longitudinal relaxation energy obtained from the empirical relationship $\ln \tau_L = \frac{H_L}{RT} + \ln b$.

[d] From ref [95].

Numbers in brackets correspond to the relevant reference.

Table 2. Characteristic energies of the of the TEMPO/TEMPO$^+$ self-exchange in pure solvents at 293K

3. Spin exchange reactions

Spin exchange and its effect on the acquired ESR spectra is well understood, experimentally as well as theoretically [108-115]. A large amount work has been done using nitroxide radicals, e.g. by Plachy and Kivelson who studied the spin exchange between di-tertiary-butyl nitroxide radicals in n-pentane and propane [116]. Another interesting work is one of Bales, where the spin exchange between various nitroxide radicals was used to study the structure of micelles as well as chemical reactions taking place within them [117].

Other authors have studied intramolecular spin exchange in nitroxide biradicals [118-122] or the so-called paramagnetic exchange between a nitroxide radical and a paramagnetic line broadening agent [123-126]. Several reports have been given on temperature and pressure dependent spin exchange reactions [33, 42-45].

Due to the wealth of information available on spin exchange of nitroxide radicals, here, focus shall be on the pressure dependence of the spin exchange reaction, as this arguably has received the least attention in the past.

3.1. Theory of pressure dependent spin exchange

With respect to the pressure dependence of the spin exchange reaction, an approach similar to the one shown for self-exchange can be made. Thus, the activation volume takes the form shown below, containing contributions from diffusion, Coulombic work and Debye-Hückel effects.

$$\Delta^{\ddagger}V_{calc} = \Delta^{\ddagger}V_{diff} + \Delta^{\ddagger}V_{Coulomb} + \Delta^{\ddagger}V_{DH} - RT\beta \tag{42}$$

$\Delta^{\ddagger}V_{Columb}$ and $\Delta^{\ddagger}V_{DH}$ can be calculated as shown above and $\Delta^{\ddagger}V_{diff}$ is obtained analogously to equation (29):

$$\Delta^{\ddagger}V_{diff} = -RT\left(\frac{\partial \ln k_{diff}}{\partial P}\right)_T \tag{43}$$

The expression of k_{diff} varies with the used theoretical description of diffusion, but often a simple Smoluchowski approach, as above, is sufficient. The last term in eq. 5 takes into account the compression of the solvent due to elevated pressures and typically has a value of 1 – 3 cm^3/mol.

3.2. Experimental results

Spin exchange rate constants, $k_{obs} = k_{se}$, obtained in some pressure dependent studies are shown in table 3 together with the corresponding activation volumes for spin exchange and diffusion.

From the pressure dependent rate constants, volumes of activation were determined for each system according to equation (29).

The differences between the values of $\Delta^{\ddagger}V_{exp}$ and $\Delta^{\ddagger}V_{diff}$ vary tremendously with the solvent and radical used. Several explanations for this have been offered. For example, it was noted in [43] that for non-polar solvents, the agreement between the volumes is very good, whereas it fails for protic polar solvents. The explanation for this is suggested to lie in the formation of the encounter complex prior to the spin exchange. If the solvent assists in this, e.g. through hydrogen bonds, a noticeable reduction in the experimental activation volume is to be expected.

The theoretical description of k_{se} has been thoroughly dealt with in literature [108, 109]. relating it to the diffusional rate constant, k_{diff}, by

$$k_{se} = pf_S k_{diff} \tag{44}$$

where p is the probability of spin exchange upon collision of the radicals and f_S is a steric factor that takes into account the anisotropy of the spin exchange, i.e., its dependence on the orientation of the colliding particles.

Compound	Solvent	k_{se} / 10^9 l mol^{-1} s^{-1}	$\Delta^{\ddagger}V_{exp}$ / cm^3 mol^{-1}	$\Delta^{\ddagger}V_{diff}$ / cm^3 mol^{-1}
TEMPO	Acetone [44]	7.8	10.7	15.8
	Acetonitrile [95]	3.9±0.3	9.4±0.7	8,1
	Methanol [95]	2.8±0.2	8.5±0.9	8.8
4-hydroxy-TEMPO	Acetone [45]	6.42	8.1	15.8
	n-Hexane [45]	10.7	13.3	23.2
4-oxo-TEMPO	Acetone [44]	8.1	8.7	15.8
	n-Hexane [44]	11.5	12.1	23.2
	Methanol [42]	5.5±0.2	6.7±1.1	8.8
	Water [42]	1.9±0.1	-7.6±0.4	-2.5
	Benzene [43]	5.3±0.3	18.4±1.0	19.1
	Toluene [42]	5.27±0.09	13.7±0.9	14.2
	o-Xylene [43]	4.2±0.2	15.3±1.2	15.5
4-amino-TEMPO	Acetone [45]	5.82	12.6	15.8
	n-Hexane [45]	8.94	11.5	23.2
DTBN	Acetone [44]	9.4	7.4	15.8

Numbers in brackets correspond to the relevant reference.

Table 3. Rate constants and activation volumes of selected spin exchange reactions.

The probability factor can be determined as shown in equation (45), using the exchange integral, J, and the collision time τ_1 as well as a factor p_{max} which depends on the value of the spin and the spin-lattice relaxation time of the radical [108].

$$p = p_{max} \frac{J^2 \tau_1^2}{1 + J^2 \tau_1^2} \tag{45}$$

The pressure dependence of the probability factor has been shown to differ from one solvent to another [44]. For many solvents, p is practically pressure independent while for others, such as acetone or hexane, it varies greatly with pressure. This is believed to be connected to the strength of the exchange. Systems with a pressure independent p, are believed to exhibit strong exchange, i.e. p≈1, whereas those showing a pressure dependent p are in the weak exchange region. This illustrates the large discrepancies between $\Delta^{\ddagger}V_{exp}$ and $\Delta^{\ddagger}V_{diff}$ in those solvents.

For reactions where the spin exchange is realised by the use of a paramagnetic broadening agent, the situation is similar. Some data obtained from this kind of experiments are shown in table 4.

Compound	Solvent	k_{se} /10^9 l mol^{-1} s^{-1}	$\Delta^{\ddagger}V_{exp}$ / cm^3 mol^{-1}	$\Delta^{\ddagger}V_{diff}$ / cm^3 mol^{-1}
	Tetrahedral complexes			
4-oxo-TEMPO /[CoCl2(solv)2]	1-Propanol [127]	1.42	15.1	16.4
	1-Butanol [127]	0.95	24.4	20.7
	1-Pentanol [127]	0.75	4.4	9.5
4-oxo-TEMPO /[CoBr2(solv)2]	1-Propanol [127]	1.75	16.6	16.4
10-DOXYL /[CoCl2(solv)2]	1-Propanol [127]	4.22	1.3	16.4
	Octahedral complexes			
4-oxo-TEMPO /[Co(acac)2(C5H5N)2]	1-Propanol [127]	3.06	-0.2	16.4
4-oxo-TEMPO /[Co(acac)2(C5H5N)2]	Chloroform [127]	1.88	-0.7	9.9
4-oxo-TEMPO /[Ni(acac)2(C5H5N)2]	Chloroform [127]	1.15	-0.2	9.9
DTBN /[Co(acac)2(C5H5N)2]	Chloroform [127]	5.03	-1.2	9.9
DTBN /[Ni(acac)2(C5H5N)2]	Chloroform [127]	2.46	0.3	9.9
TEMPO /Fe(acac)3	Methanol [128]	4.4±0.4	12.2	8.8
	Acetone [128]	7.7±0.7	13.6	15.8
	Chloroform [128]	3.2±0.3	11.8	9.9

Numbers in brackets correspond to the relevant reference.

Table 4. Rate constants and activation volumes of selected paramagnetic exchange reactions.

When the paramagnetic exchange takes place between a nitroxide and a tetragonal transition metal complex, only slight differences between $\Delta^{\ddagger}V_{exp}$ and $\Delta^{\ddagger}V_{diff}$ are observed, thus indicating strong exchange. An exception is the reaction between 10-DOXYL and $[CoCl_2(C_3H_7OH)_2]$, where the steric hindrance around the >N-O$^{\bullet}$ group leads to weak exchange.

However, changing the structure of the complex to orthogonal, a change in the effectiveness of the paramagnetic exchange is observed. The steric hindrance is now increased and many complexes show weak exchange.

4. Conclusion

ESR is a suitable tool for investigating the kinetics and thermodynamics of exchange reactions. Such reactions are often used to model elementary processes like electron transfer and diffusion. Electron Self- and spin exchange rate constants can be measured quite accurately and from their temperature and pressure dependencies, the corresponding activation energies and volumes can be determined. The obtained experimental data may be interpreted within the framework of the appropriate theories, e.g. Marcus theory in the case of electron transfer.

Due to their great stability and the relative simplicity of their ESR spectra, nitroxides are prime candidates in ESR line broadening experiments.

Author details

Günter Grampp and Kenneth Rasmussen
Institute of Physical and Theoretical Chemistry, Graz University of Technology, Graz, Austria

Acknowledgement

The authors would like to thank Dr. A. Kokorin for helpful discussion through many years. The collaboration of Dr. T. Hussain, Dr. D. Kattnig, Dr. B. Mladenova-Kattnig and Dr. S. Landgraf is also greatly appreciated.

Financial supports are acknowledged from different foundations: The German Science Foundation (DFG), the Volkswagen-Foundation (Hanover, Germany), the Austrian Science Foundation (FWF), the WTZ-programs from the Austrian Exchange Service (OeAD) and the Asea-Uninet Network Program for travel grants.

5. References

[1] Grampp G (1998) Intermolecular Electron-Self Exchange Kinetics Measured by Electron Paramagnetic Resonance-Linebroadening Effects: Useful Rate Constants for the Application of Marcus Theory. Spectrochim. Acta A. 54A: 2349-2358.
[2] G. Grampp and D. Kattnig, to be published.
[3] Freed J H (1967) Theory of Saturation and Double Resonance Effects in Electron Spin Resonance Spectra. II. Exchange *vs.* Dipolar Mechanisms. J. Phys. Chem. 71: 38-51.
[4] Hyde J S, Pasenkiewicz-Gierula M, Jesmanowicz A and Antholine W E (1990) Pseudo Field Modulation in EPR Spectroscopy. Appl. Magn. Reson. 1: 483-496.
[5] Weil J A, Bolton J R (2007) Electron Paramagnetic Resonance, Elementary Theory and Practical Applications. New York: Wiley-Interscience. 664 p.
[6] Poole C P (1996) Electron Spin Resonance, A Comprehensive Treatise on Experimental Techniques. New York: Dover Publications. 780 p.

[7] Dalal P D, Eaton S S, Eaton R E (1981) The Effects of Lossy Solvents on Quantitative EPR Studies. J. Magn. Reson. 44: 415-428
[8] Eremets M. (Ed.), (1996) High Pressure Experimental Methods. New York: Oxford University Press. 390 p.
[9] Holzapfel, W. B., Isaacs N.S.(Eds.) (1997) High-Pressure Techniques in Chemistry and Physics - The Practical Approach in Chemistry. New York: Oxford University Press. 388p.
[10] Eldik van R., Klärner F.-G. (Eds.)(2002) High Pressure Chemistry. Weinheim: Wiley-VCH. 458 p.
[11] Gaarz U, Lüdemann H.-D (1976) Ber. Bunsenges. Phys. Chem. 80: 607-614.
[12] Yamada H (1974) Pressure-resisting Glass Cell for High Pressure, High Resolution NMR Measurements. Rev. Sci. Instrum. 45: 640-642.
[13] Zahl A, Igel P, Weller M van Eldik R (2004) A High-pressure MNR Probehead for Measurements at 400 MHz. Rev. Sci. Instrum. 75: 3152-3157.
[14] Walch W M Jr. and Bloembergen M (1957) Paramagnetic Resonance of Nickel Fluosilicate under High Hydrostatic Pressure. Phys. Rev. 107: 904-905.
[15] Jaworski M, Checinski K, Bujnowski W, Porowski S (1978) High-pressure EPR Cavity. Rev. Sci. Instrum. 49: 383-384.
[16] Stankowski J, Galezewski A, Krupski M, Waplak S, Gierszal H (1976) Microwave Resonators for EPR studies ar Hgh Hydrostatic Pressure. Rev. Sci. Instrum. 47: 128-129.
[17] Sakai N, Piler H J (1985) Electron paramagnetic Resonance at High Pressure using a Diamond Anvil Cell. Rev. Sci. Instrum. 56: 726-731.
[18] Cecv P, Srinivasan R (1978) Microwave Cavity for EPR at High Pressure. Rev. Sci. Instrum. 49: 1282-1284.
[19] Bromberg S E, Chan I Y (1992) Enhanced Sensitivity for High-pressure EPR using Dielectric resonators. Rev. Sci. Instrum. 63: 3670-3673.
[20] Rupp W L Jr., Peercy P S, and Walsh W M Jr. (1977) Moderate Pressure, Low-Temperature Microwave Spectrometer. Rev. Sci. Instrum. 48: 877-878.
[21] Wu R K, Dutton T F, Doyle W T (1979) 20-Kilobar Pressure System. Rev. Sci. Instrum. 50: 586-589.
[22] Doyle W T, Dutton T F, Wolbarst A B (1972) High Prerssure ENDOR Cavity. Rev. Sci. Instrum. 43: 1668-1670.
[23] Wu R K, Dutton T F, Doyle W T (1979) K-band High-pressure Cell for ENDOR Studies. Rev. Sci. Instrum. 50: 590-594.
[24] Plachy W Z, Schaafsma T J, Wu R K, Dutton T F, Doyle W T (1969) Microwave Helices in Electron Spin Resonance Studies at High Pressure or Very Stable Temperatures. Rev. Sci. Instrum. 40: 1590-1594.
[25] Yoshioka H, Kazama S, Mitani T, Horigome T (1985) Construction of a High-Pressure Electron Spin Resonance Spectrometer Using a Helix Resonator. Anal Chem. 57: 2517-2519.
[26] Sueishi Y, Yamamoto S, Nishimura N (1993) Pressure-resisting glass cell for high-pressure ESR Measurements. Meas. Sci. Technol. 4: 1171-1172.

[27] Livingston R, Zeldes H (1981) Apparatus to Study the Electron Spin Resonance of Fluids under High Pressure Flowing at High Temperature. Rev. Sci. Instrum. 52: 1352-1357.

[28] Grandy D W, Petrakis L (1980) A High-Pressure, High-Temperature Electron Paramagnetic Resonance Cavity. J. Magn. Reson., 41: 367-373.

[29] Sienkiewicz A, Jaworski M, Garaj S, Forro L, . Scholes C P (2002) Application of Electron Spin resonance in Biophysics: From rapid Mixing Stopped-Flow to High-Hydrostatic Pressure ESR.Defect and Diffusion Forum, 208-209: 1-18.

[30] Cannistraro S (1984) Simple System for High-Pressure EPR Measurements on Aqueous Samples. Rev. Sci. Instrum., 55: 996-997.

[31] Alaeva T E, Vereshagin L F, Gvozdev V V, Timofeev U A, Shanditsev V A, Yakovlev E H (1972)A cell for the investigation of electron resonance spectra under quasi-hydrostatic pressures up to 100 kbar. Instr. Exp. Techn. 5: 206-208

[32] Filippov A I, Yablokov U V (1971) A cell to EPR spectrometer for the study of substances under hydrostatic pressures. Instr. Exp. Techn. 6: 161-164

[33] Edelstein N, Kwok A, Maki A H (1964) Effects of Hydrostatic Pressure and Temperature on Spin Exchange between Free Radicals in Solution. J. Chem. Phys. 41: 3473-3478.

[34] Edelstein N, Kwok A, Maki A H (1964) Effects of Hydrostatic Pressure on Linewidths of Free Radicals in Solution. I. Anisotropic Region. J. Chem. Phys., 41:179-183 (1964).

[35] Griller D (1978) High Pressure Electron Paramagnetic Resonance Experiments. Effect of Solvent Contraction on Hyperfine Splitting. J. Am. Chem. Soc. 100 :5240-5241.

[36] Hwang J W, Rao K V S, Freed H J (1976) An electron Spin Resonance Study of the Pressure Dependence of Ordering and Spin Relaxation in a Liquid Crystalline Solvent. J. Phys. Chem. 80: 1490-1501.

[37] Böddeker W K, Lang G, Schindewolf D U (1969) ESR Measurem,ents under Pressure: Effect of Pressure on Chemical Equilibria involving Solvated Electrons. Angew. Chem. Internat Edit. 8:138-139.

[38] Hwang J, Kivelson D, Plachy W (1973)ESR Linewitdths in Solution. VI. Variation with Pressure and Study of Functional Dependence of Anisotropic Interaction Parameter κ. J. Chem. Phys. 58: 1753-1765.

[39] Yoshioka H, Kazama S, Mitani T, Horigome T (1985) Construction of a High-Pressure Electron Spin Resonance Spectrometer Using a Helix Resonator. Anal. Chem., 57: 2517-2519.

[40] M. Kasahara, Sueishi Y, Yamamoto S (2001) Pressure Effects on Cation Migration in 2,5-Di-tert-Butyl-1,4-Benzoquinone Radical Anion. Int. J. Chem. Kinet. 33: 397-401.

[41] Sueishi Y, Kuwata K (1989) Pressure Effects on the Electron Spin Relaxation of Several Radicals in Solution. Chem. Phys. Lett., 160: 640-643.

[42] Sueishi Y, Nishimura N, Hirata K, Kuwata K (1988) ESR Studies of Solvent and Pressure Effects on Spin Exchange of Nitroxide Radicals in Solution. Bull. Chem. Soc. Jpn., 61: 4253-4257.

[43] Sueishi Y, Nishimura N, Hirata K, Kuwata K (1990) ESR Studies at high Pressure II. Spin Exchange of 2,2,6,6-Tetramethyl-4-oxo-1-piperidininyoxyl in Protic and Aprotic Solvents. Bull. Chem. Soc. Jpn.63, 252-254.

[44] Sueishi Y, Kuzukawa M, Yamamoto S, Nishimura N (1991) ESR Studies at high Pressures.III. Spin-Exchange Reactions of Some Nitroxide Radicals in Acetone and Hexane. Bull. Chem. Soc. Jpn., 64: 2188-2191.

[45] Sueishi Y, Kuzukawa M, Yamamoto S, Nishimura N (1992) ESR Studies at high Pressure. IV. Spin-exchange Reactions in various Types of Nitroxides in Some Low-Viscosity Solvents. Bull. Chem. Soc. Jpn. 65: 3118-3121.

[46] Sueishi Y, Kasahara M, Kotake Y (2000) Differential Pressure Effect on Bimodal Inclusion Complex of β-Cyclodextrin with a Nitroxide Probe as Studies with Electron Paramagnetic Resonance. Chem. Lett. 792.

[47] Sueishi Y, Nishimura N, Hirata K, Kuwata K (1991) An ESR Study of Pressure Effects on the Inclusion-Complex Formation ov cyclodextrins with Di-tert-butyl Nitroxide. J. Phys. Chem. 95: 5359-5361.

[48] Sueishi Y, Noritake K, Liu Y J (1999), An EPR Study on Intramolecular Spin Exchange and Rotational Mobility of Nitroxides Linked with a Long Chain. Chemical Research in Chinese Universities, 15: 174-181.

[49] Sueishi Y, Nishimura N (1993) High Pressure Electron spin resonance of radicals in Solution , Koatsuryoku no Kagaku to Gijutsu, 2: 139-145.

[50] Goldhammer E, Paul J, Wenzel H R (1992) Applications of Spin-Label Techniques at High Pressure. In: Zhdanov R I, editor. Bioact. Spin Labels .Berlin: Springer. pp.611-629.

[51] McCoy J, Hubbell L W (2011) High-pressure EPR reveals Conformational Equilibria and Volumetric Properties of Spin-Labeled Proteins. PNAS 108: 1331-1336.

[52] Pfund D M, Zemanian T S, Linehan J C, Fulton J L, Yonker C R (1994) Fluid Structure in Supercritical Xenon by Nuclear magnetic Resonance Spectroscopy and Small Angle Y-Ray Scattering. J.Phys.Chem. 98:11846-11857.

[53] Rasmussen K, Hussain T, Landgraf S, Grampp G (2012) High Pressure ESR Studies of Electron Self-Exchange Reactions of Organic Radicals in Solution. J. Phys. Chem. 116: 193-198.

[54] Ward R L, Weissman S I (1957) Electron Spin Resonance Study of the Electron Exchange between Naphthalene Negative Ion and Naphthalene. J. Am. Chem. Soc. 79: 2086-2090.

[55] Zandstra P J, Weissman S I (1961) Note on Measurements of Rates of Electron Transfer Processes by Broadening of ESR Lines. *J. Chem. Phys*. 35: 757

[56] Layloff T, Miller T, Adams R N, Fah H, Horsfield A, Proctor W (1965) Homogeneous Electron Exchange Reactions of Aromatic Molecules. Nature 205: 382-383.

[57] Malachesky P A, Miller T A, Layloff T, Adams R N (1965) Electron-exchange reactions of aromatic molecules. *Exchange Reactions Proc. Symp., Upton, N.Y.*: 157-170.

[58] Marcus R A (1956) On the Theory of Oxidation-Reduction Reactions Involving Electron Transfer. I. J. Chem. Phys. 24: 966-978.

[59] Marcus R A (1957) On the Theory of Oxidation-Reduction Reactions Involving Electron Transfer. II. Applications to Data on the Rates of Isotopic Exchange Reactions. J. Chem. Phys. 26: 867-871.
[60] Marcus R A (1957) On the Theory of Oxidation-Reduction Reactions Involving Electron Transfer. III. Applications to Data on the Rates of Organic Redox Reactions. J. Chem. Phys. 26: 872-877.
[61] Bixon M, Jortner J (1993) Solvent Relaxation Dynamics and Electron Transfer. Chem. Phys. 176: 467-481.
[62] Hush N S (1961) Adiabatic theory of outer sphere electron-transfer reactions in solution. Trans. Faraday Soc. 57: 557-580.
[63] Sumi H, Marcus R A (1986) Dynamical Effects in Electron Transfer Reactions. J. Chem. Phys. 84: 4894-4914.
[64] Holstein T (1978) Quantal Occurrence-Probability Treatment of Small-Polaron Hopping. Philos. Mag. B 37: 49-62.
[65] Jortner J, Bixon M (1988) Intramolecular Vibrational Excitations Accompanying Solvent-Controlled Electron Transfer Reactions. J. Chem. Phys. 88: 167-170.
[66] Sutin N (1983) Theory of Electron Transfer Reactions: Insights and Hindsights. Prog. Inorg. Chem. 30: 441-498.
[67] Nelsen S F, Newton M D (2000) Estimation of Electron Transfer Distances from AM1 Calculations. J. Phys. Chem. A. 104: 10023-10031.
[68] Nelsen S F, Blackstock S C, Kim Y (1987) Estimation of Inner Shell Marcus Terms for Amino Nitrogen Compounds by Molecular Orbital Calculations. J. Am. Chem. Soc. 109: 677-682.
[69] Grampp G, Jaenicke W (1991) Kinetics of Diabatic and Adiabatic Electron Exchange in Organic Systems Comparison of Theory and Experiment. Ber. Bunsenges. Phys. Chem. 95: 904-927.
[70] Clegg A D, Rees N V, Klymenko O V, Coles B A, Compton R G (2004) Marcus Theory of Outer-Sphere Heterogeneous Electron Transfer Reactions: Dependence of the Standard Electrochemical Rate Constant on the Hydrodynamic Radius from High Precision Measurements of the Oxidation of Anthracene and Its Derivatives in Nonaqueous Solvents Using the High-Speed Channel Electrode. J. Am. Chem. Soc. 126: 6185-6192.
[71] Rees N V, Clegg A D, Klymenko O V, Coles B A, Compton R G (2004) Marcus Theory for Outer-Sphere Heterogeneous Electron Transfer: Predicting Electron-Transfer Rates for Quinones. J. Phys. Chem. B. 108: 13047-13051.
[72] German E D, Kuznetsov A M (1981) Outer Sphere Energy of Reorganization in Charge Transfer Processes. Electrochim. Acta 26: 1595-1608.
[73] German E D, Kharkats I Yu (1995) Calculation of the polar media reorganization energy for the model of two dielectric spheres. Chem. Phys. Lett. 246: 427-430.
[74] Marcus R A (1965) On the Theory of Electron-Transfer Reactions. VI. Unified Treatment for Homogeneous and Electrode Reactions. J. Chem. Phys. 43: 679-701.
[75] Kramers H A (1940) Brownian Motion in a Field of Force and the Diffusion Model of Chemical Reactions. Physica 7: 284-304.

[76] Zusman L D (1988) The Theory of Electron Transfer Reactions in Solvents with two Characteristic Relaxation Times. Chem. Phys. 119: 51-61.
[77] Zusman L D (1994) Dynamical Solvent Effects in Electron Transfer Reactions. Z. Phys. Chem. 186: 1-29.
[78] Rips I, Jortner J (1987) Dynamic Solvent Effects on Outer-Sphere Electron Transfer. J. Chem. Phys. 87: 2090-2104.
[79] Rips I, Jortner J (1987) Outer Sphere Electron Transfer in Polar Solvents. Activationless and Inverted Regimes. J. Chem. Phys. 87: 6513-6519.
[80] Fröhlich H (1958) Theory of Dielectrics: Dielectric Constant and Dielectric Loss. Oxford: Claredon Press. 192 p.
[81] Zusman L. D (1980) Outer-Sphere Electron Transfer in Polar Solvents. Chem. Phys. 49: 295-304.
[82] Zusman L D (1983) The Theory of Transitions between Electronic States. Application to Radiationless Transitions in Polar Solvents. Chem. Phys. 80: 29-43.
[83] Weaver M J (1992) Dynamical Solvent Effects on Activated Electron-Transfer Reactions: Principles, Pitfalls, and Progress. Chem. Rev. (Washington, DC, United States). 92: 463-480.
[84] Weaver M J, McManis G E III (1990) Dynamical Solvent Effects on Electron-Transfer Processes: Recent Progress and Perspectives. Acc. Chem. Res. 23: 294-300.
[85] Barthel J, Buchner R, Hölzl C G, Münsterer M (2000) Dynamics of Benzonitrile, Propylene Carbonate and Butylene Carbonate: the Influence of Molecular Shape and Flexibility on the Dielectric Relaxation Behaviour of Dipolar Aprotic Liquids. Z. Phys. Chem. 214: 1213-1231.
[86] Swaddle T W (1990) "Pressure-Testing" Marcus-Hush Theories of Outer-Sphere Electron-Transfer Kinetics. Inorg. Chem. 29: 5017-5025.
[87] Swaddle T W (1996) Reflections on the Outer-Sphere Mechanism of Electron Transfer. Can. J. Chem. 74: 631-638.
[88] Zahl A, van Eldik R, Matsumoto M, Swaddle T W (2003) Self-Exchange Reaction Kinetics of Metallocenes Revisited: Insights from the Decamethylferricenium − Decamethylferrocene Reaction at Variable Pressure. Inorg. Chem. 42: 3718-3722.
[89] Stranks D R (1974) The Elucidation of Inorganic Reaction Mechanisms by High Pressure Studies. Pure Appl. Chem. 38: 303-323.
[90] Zhdanov R I, Golubev V A, Gida, V M (1971) Interaction of iminoxyl radicals with antimonypentachloride. Proc. Acad. Sci. USSR 196: 856-857.
[91] Miyazawa T, Endo T, Shiihashi S (1985) Selective oxidation of alcohols by oxoammonium salt ($R_2N = O^+X^-$). J. Org. Chem. 50: 1332-1334
[92] Liu Y C, Ding Y B, Liu Z L (1990) Preparation of single crystal and molecular structure of phenothiazine radical cation hexachloroantimonates. Acta Chimica Sinica 48: 1199-1203
[93] Wu L, Guo X, Wang J, Guo Q, Liu Z, Liu Y (1999) Kinetic Studies on the Single Electron Transfer Reaction between 2,2,6,6-Tetramethylpiperidine Oxoammonium Ions and Phenothiazines: the Application of Marcus Theory. Sci. China Ser. B 42: 138-144.

[94] Grampp G, Landgraf S, Rasmussen K, Strauss S (2002) Dimerization of Organic Free Radicals in Solution.: 1. Temperature Dependent Measurements. Spectrochim. Acta A 58A: 1219-1226.

[95] Rasmussen K, (2006) High-Pressure ESR Spectroscopy Applied to the Kinetics of Electron Self-Exchange Reactions in Solution. Dissertation, Graz University of Technology

[96] Mansingh K, Mansingh A (1964) Dielectric relaxation and viscosity of liquids. Ind. J. Pure Appl. Phys. 2: 176-178.

[97] Owen B B, Miller R C, Milner C E, Cogan H L (1961) The Dielectric Constant of Water as a Function of Temperature and Pressure. J. Phys. Chem. 65: 2065-2070.

[98] Barthel J, Buchner R, Munsterer M (1996) Electrolyte Data Collection. Part 2a Dielectric Properties of Nonaqueous Electrolyte Solutions. Frankfurt/Main: Dechema. 387 p.

[99] Buchner R, Barthel J, Stauber J (1999) The Dielectric Relaxation of Water between 0°C and 35°C. Chem. Phys. Lett. 306: 57-63.

[100] Finklea H O, Madhiri N (2008) Reorganization energies of $TEMPO^{\bullet}/TEMPO^{+}$ in water. J. Electroanal. Chem. 621: 129-133.

[101] Fawcett W R (1992) Time Dependence of the Relaxation Parameters in non-Debye Solvents. Chem. Phys. Lett. 199: 153-160.

[102] Shirke R M, Chaudhari A, More N M, Patil P B (2001) Temperature Dependent Dielectric Relaxation Study of Ethyl Acetate — Alcohol Mixtures Using Time Domain Technique. J. Mol. Liq. 94: 27-36.

[103] Shirke R M, Chaudhari A, More N M, Patil P B (2000) Dielectric Measurements on Methyl Acetate + Alcohol Mixtures at (288, 298, 308, and 318) K Using the Time Domain Technique. J. Chem. Eng. Data 45: 917-919.

[104] Simon J D (1988) Time-Resolved Studies of Solvation in Polar Media. Acc. Chem. Res. 21: 128-134.

[105] Bertolini D, Cassettari M, Salvetti G (1983) The Dielectric Properties of Alcohols–Water Solutions. I. The Alcohol Rich Region. J. Chem. Phys. 78: 365-372.

[106] Chaudhari A, Khirade P, Singh R, Helambe S N, Narain N K, Mehrotra S C (1999) Temperature dependent dielectric relaxation study of Tetrahydrofuran in Methanol and Ethanol at microwave frequency using Time Domain Technique. *J. Mol. Liq.* 82: 245-253.

[107] Carvajal C, Tolle K J, Smid J, Szwarc M (1965) Studies of Solvation Phenomena of Ions and Ion Pairs in Dimethoxyethane and Tetrahydrofuran. J. Am. Chem. Soc. 87: 5548-5553.

[108] Molin Yu N, Salikhov K M, Zamaraev K I (1980) Spin Exchange Principles and Applications in Chemistry and Biology. Berlin: Springer-Verlag. 242 p.

[109] Nayeem A, Rananavare S B, Sastry V S S, Freed J H (1989) Heisenberg Spin Exchange and Molecular Diffusion in Liquid Crystals. J. Chem. Phys. 91: 6887-6905.

[110] Berner B, Kivelson D (1979) The Electron Spin Resonance Line Width Method for Measuring Diffusion. A Critique. J. Phys. Chem. 83: 1406-1412.

[111] Bales B L, Stenland C (1995) Statistical Distributions and Collision Rates of Additive Molecules in Compartmentalized Liquids Studied by EPR. 2. Sodium Dodecyl Sulfate Micelles, 5-Doxylstearic Acid Ester, and Copper(II). J. Phys. Chem. 99: 15163-15171.

[112] Salikhov K M (2010) Contributions of Exchange and Dipole-Dipole Interactions to the Shape of EPR Spectra of Free Radicals in Diluted Solutions. Appl. Magn. Reson. 38: 237-265.

[113] Kivelson D J (1960) Theory of ESR Linewidths of Free Radicals. J. Chem. Phys. 33: 1094-1106.

[114] Currin J D (1962) Theory of Exchange Relaxation of Hyperfine Structure in Electron Spin Resonance. Phys. Rev. 126: 1995-2001.

[115] Johnson Jr, C S (1967) Theory of Line Widths and Shifts in Electron Spin Resonance Arising From Spin Exchange Interactions. Mol. Phys. 12: 25-31

[116] Plachy W, Kivelson D (1967) Spin Exchange in Solutions of di-Tertiary-Butyl Nitroxide. J. Chem. Phys. 47: 3312-3318

[117] Bales B L, Ranganathan R, Griffiths P C (2001) Characterization of Mixed Micelles of SDS and a Sugar-Based Nonionic Surfactant as a Variable Reaction Medium. J. Phys. Chem. B 105: 7465–7473

[118] Parmon V N, Kokorin A I, Zhidomirov G M (1977) Conformational Structure of Nitroxide Biradicals Use of Biradicals as Spin Probes. J. Struct. Chem. 18: 104-147.

[119] Parmon V N, Kokorin A I, Zhidomirov G M (1980) Stable Biradicals. Moscow: Nauka 240 p.

[120] Rassat A (1971) Application of Electron Spin Resonance to Conformational Analysis. Pure. Appl. Chem. 25: 623-634.

[121] Shapiro A B, Baimagambetov K, Goldfield M G, Rozantsev E G (1972) Long-chain iminoxyl biradicals. Zh. Org. Khim. 8: 2263-2269.

[122] Parmon V N, Kokorin A I, Zhidomirov G M, Zamaraev K I (1975) On the Mechanism of Spin Exchange in Long-Chain Nitroxide Biradicals. Molec. Phys. 30: 695-701.

[123] Salikhov K M, Doctorov A B, Molin Yu N, Zamaraev K I (1971) Exchange Broadening of ESR Lines for Solutions of Free Radicals and Transition Metal Complexes. J. Magn. Reson. 5: 189-205.

[124] Sueishi Y, Inoue H, Oka T, Tsukube H, Yamamoto S (1998) EPR Studies at High-Pressures. V. Spin-Exchange Reactions of Nitroxide Radicals with Cobalt and Nickel Complexes. Bull. Chem. Soc. Jpn. 71: 817-823.

[125] Sueishi Y, Hori A (2001) EPR Studies at High-Pressure. VI. Spin-Exchange Reaction of Nitroxide Radical with Copper(II) and Iron(III) Complexes. Bull. Chem. Soc. Jpn. 74: 2431-2432.

[126] Kokorin A I, Pridantsev A A (1997) Diffusion of Molecules and Ions in Solutions of Complexing Polymers. Zh. Fiz. Khim. (Russ. J. Phys. Chem. A) 71(12): 1963-1969.

[127] Sueishi Y, Inoue H, Oka T, Tsukube H, Yamamoto S (1998) EPR Studies at High-Pressures. V. Spin-Exchange Reactions of Nitroxide Radicals with Cobalt and Nickel Complexes. Bull. Chem. Soc. Jpn. 71: 817-823.

[128] Hussain T, (2009) Pressure and Temperature Dependence of Spin- and Electron-Exchange Reactions Measured by ESR Spectroscopy. Dissertation, Graz University of Technology

IntechOpen